3. RESULTS

The 3D radiation pattern of our optimized antenna is shown in Figure 3. The pattern is omni in the upside direction, with a gain around 2 dB.

From these data, we can predict the reading distance, which is shown (for different transmssion ERP, up to 3 dBW) in Figure 4. Actually, even for an ERP as low as −10 dBW (a value which comply with every national regulation) the reaching distance is larger than 1.5 m in almost all the useful bandwidth.

ACKNOWLEDGMENT

Work supported by Regione Autonoma della Sardegna, under contract Ottimizzazione della logistica in ambito sanitario attraverso l'utilizzo di sistemi RFid, No. F71J12000820002.

REFERENCES

1. Dobkin, D. M., *The RF in RFID: Passive UHF RFID in Practice*, Newnes, 2007.
2. Sani, M. R., R. Foster, and Y. Hao, "Antennas and propagation of implanted RFIDs for pervasive healthcare applications," *Proceedings of the IEEE*, 1648–1655, Sep. 2010.
3. Borrelli, G., F. V. Caredda, A. Fanti, G. Gatto, G. Mazzarella, P. F. Orr, A. Serpi, I. L. Spano, E. Tanzi, A. Volpi, and F. Zedda, "Preliminary study of RFID technologies for health-care applications," *The Internetional Workshop on Innovative Simulation for Healthcare*, Sep. 2014.
4. Dubok, T., T. J. Coenen, A. Zamanifekri, and A. B. Smolders, "Robust UHF RFID antennas in complex environments," *7th European Conference on Antennas and Propagation (EuCAP)*, 1695–1699, Apr. 2013.
5. Ibrahim, R. A. and M. C. E. Yagoub, "Pratical novel design component of microstrip patch slot antenna MSPSA for RFID applications," *IEEE 23rd Canadian Conference on Electrical and Computer Engineering (CCECE)*, May 2010.
6. Marrocco, G., "RFID antennas for the UHF remote monitoring of human subjects," *IEEE Transactions on Antennas and Propagation*, Jun. 2007.
7. Franceschetti, G., *Electromagnetics: Theory, Techniques, and Engineering Paradigms*, Plenum Press, 2013.
8. Fanti, F., R. Secci, G. Boi, S. Casu, G. A. Casula, G. Mazzarella, and G. Montisci, "A polycarbonate RFID tag for blood chain tracking," *Antennas Propagation Symposium*, Vancouver, Jul. 2015.
9. CST GmbH, CST Microwave Studio Help, CST Studio Suite Version 2011.14.01, 2011, http://eee. guc.edu.eg/Courses/Communications/COMM905.

28 GHz Delay Spread Measurement Using a Broadband Channel Sounder in Small Urban City

Young Keun Yoon, **Jong Ho Kim**, **Myoung Don Kim**,
Young Jun Chong, **and Myoung Sun Song**
ETRI (Electronics and Telecommunications Research Institute), Republic of Korea

Abstract— This paper describes the relations between the R.M.S delay spread and TX-RX separation distance for Daejeon City measurements at 28 GHz frequency with 500 MHz channel bandwidth. R.M.S delay spread is caused by multipath due to a large number of reflective and diffractive characteristics in various urban environments.

1. INTRODUCTION

Recently, the fifth generation mobile communication to satisfy the needs of high data rates in the small cell environment has attracted the attention. Millimeter frequency bands for 5G services are the lands of new frontier being able to support broadband bandwidth from 0.5 up to 2.0 GHz in [1]. We know that feasibility research at millimeter bands is carried out currently. Yet, there is still the lack of the collected field data and statistical models based on measurement. Therefore, we performed measurement in small urban city of Korea to find specific root mean square delay spread characteristics.

2. HARDWARE & MEASUREMENT CAMPAIGN

2.1. Hardware Channel Sounder

Millimeter wave Band Exploration and Channel Sounder (mBECS) developed by Electronics and Telecommunications Research Institute (ETRI) was used in the indoor/outdoor both pathloss and root mean square (R.M.S) delay spread measurement campaign. mBECS is a wideband channel sounder for measuring temporal and spatial characteristics. Using a 500 Mcps broadband channel sounder with 2.0 ns multipath resolution, we conducted R.M.S delay spread measurements at 28 GHz frequency band in Daejeon City, Korea. mBECS consists of five parts: baseband/IF modules, RF module, horn antenna, timing module and mechanical module. A measurement manager is able to control each part of the transmitter (TX) and receiver (RX). Timing module operates as rubidium oscillator which provides reference clock within 1ns in order to synchronize the clock of TX and RX being far away. A 4095 chips pseudo-random noise (PN) sequence sliding correlator was utilized, which was modulated to a 5.2 GHz intermediate frequency (IF) and upconverted 28 GHz. The maximum TX power was 29 dBm, fed to a 30° beamwidth 12.9 dBi horn antenna that was mechanically rotated or tilted. The RX used a 10° beamwidth 21.4 dBi horn antenna and the same type of enable mechanically rotating or tilting structure such as the transmitter with antennabeamwidth of 30°.

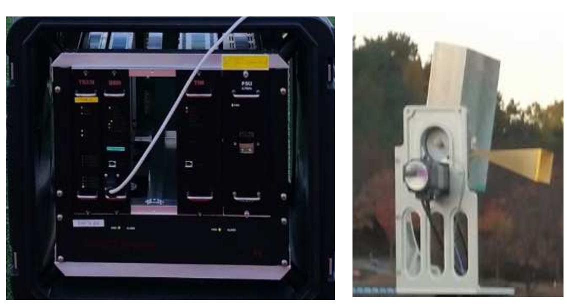

(a) (b)

Figure 1: Channel sounder. (a) Baseband/IF module. (b) RF/antenna/positioner.

2.2. Measurement Campaign

To obtain delay spread characteristics in none line of sight(NLOS) environment, TX site locates on the side of a four-lane main road in the Daejeon City of Korea. NLOS environmentincludes low-rise (three to five stories which has nine to fifteen meter height) buildings, a four-lane main road, several two-lane side streets, vehicles, subsidiary facilities, and peoples. The measurement campaign was taken during daytime from 9 am to 6 pm. During measurement, TX location and antenna bore sight direction was fixed, and RX puts in two-lane side load in NLOS locations. We choose one TX at a height of 4 m and 15 RX measurement locations. The distance between the TX and RX ranged from about 120 to 400 m. At RX at a height of 1.5 m, a 360° azimuth sweep at each RX positionwas automatically performed in steps of 10° because of using 21.4 dBi horn antenna with the 10° half power beamwidth. Extensive measurements were conducted for the thirty six different RX azimuth angles ranged from 0° to 350° , and for the three different RX elevation angles of −10° , 0°, and +10° creating one hundred eight possible antenna pointing steps. For each of one hundred eight steps, measurement data were recorded. Finally, R.M.S delay spread measurements were done at the RX locations in Daejeon, Republic of Korea

Figure 2: Measurement campaign.

3. RESULTS

3.1. Delay Spread

Multipath, which results in intersymbol interference, causes time dispersion, as described by channel impulse response (CIR). When channel is time varying, time t is needed, and τ is multipath delay.

Let equivalent complex-envelop CIR in time-variant is,

$$h(t\tau) = \sum_{i=0}^{I-1} p_i\,(t,\tau)\exp\left(-j\varphi_i\,(t,\tau)\right)\delta(\tau - \tau_i(t)) \quad (1)$$

where, p_i, φ_i, τ_i are theamplitude, phase shift and excess delay of the i-th propagation path, respectively. I means total multipath components of transmitted signal arriving at RX. Useful to discrete τ into delay bins, each bin represents a multipath component. At time t, each bin arrives at RX with different amplitude, go through a different phase shift, and has a different excess delay.

To derive delay spread at RX in this paper, it is assumed that channel is time invariant as a special case. This means that multipath components of transmitted signals arriving at the same RX location have the same time excess delay. In time-invariant case, let equivalent complex-envelop CIR can be written as,

$$h(\tau) = \sum_{i=0}^{I-1} p_i \exp\left(-j\varphi_i\right)\delta(\tau - \tau_i) \quad (2)$$

where, p_i, $\varphi_i\tau_i$ are theamplitude (Rayleigh distributed), phase shift (uniformly distributed) and excess delay (Poisson distributed) of the i-th propagation path, respectively.

R.M.S delay spread ($\tau_{R.M.S}$), which is defined as the square root of the second central moment of power delay profile, is a measurement index of multipath which results in inter-symbol interference

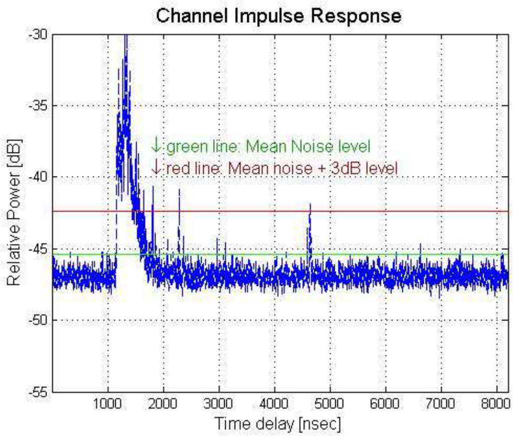

Figure 3: Power delay profile.

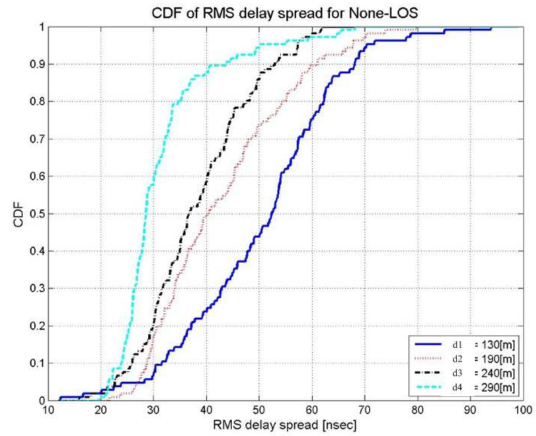

Figure 4: Delay Spread: CDF.

to communication system. With $\tau_0 = 0$, it is given by,

$$\tau_{R.M.S} = \sqrt{\frac{\sum_{i=0}^{I-1} \tau_i^2 \cdot P(\tau_i)}{\sum_{i=0}^{I-1} P(\tau_i)} - \tau_a^2} \tag{3}$$

with

$$\tau_a = \frac{\sum_{i=0}^{I-1} \tau_i P(\tau_i)}{\sum_{i=0}^{I-1} P(\tau_i)} \tag{4}$$

where, τ_a is mean excess delay, which is defined as the first moment of power delay profile, $P(\tau_i)$ is the channel power spectral density as a function of a delay, i.e., how channel power is distributed along dimension excess delay.

3.2. Analysis

We note that the maximum value of R.M.S delay spread appears to be up to 400 m TX-RX separation distance at 28 GHz frequency, and then decreases for relative large TX-RX separation distance. In NLOS case, the TX and RX antennas were indirectly pointed at each other, and large multipath existed. But, when the separation distance between a TX and Rx is too large (exceeding 400 m) in NLOS, the pathloss is so great that the power of the transmitted signal declines to zero before reaching the RX, resulting in fewer or no received multipath. For the relations between the R.M.S delay spread and TX-RX separation distance as well as the cumulative distribution function (CDF) of the R.M.S delay spread at 28 GHz, the maximum value of measured multipath components using wide band channel sounder with 2.0 ns multipath time resolution has R.M.S delay spreads below 125 ns, the average has below 58 ns to NLOS environments in small commercial urban environment of Daejeon, Republic of Korea.

4. CONCLUSION

We found that the measured values from the light urban environment of Daejeon City in Republic of Korea have substantial differences in comparison with the dense urban environment in R.M.S delay spread in [2]. To find adequate R.M.S delay spread components, we believe that the results through extensive measurement in various urban environments should be more discussed.

ACKNOWLEDGMENT

This work was supported by Institute for Information & communications Technology Promotion (IITP) grant funded by the Korea government (MSIP). [B0101-15-222, Development of core technology to improve spectral efficiency for mobile big-bang].

REFERENCES

1. Fallgren, M. and B. Timus, "Deliverabble d1.1 scenarios, requirements and kpis for 5g mobile and wireless system," *METIS*, Document Number: ICT-317669-METIS/D1.1, Tech. Rep., 2013.
2. Rappaport, T., S. Sun, R. Mayzus, H. Zhao, Y. Azar, K. Wang, J. Schulz, M. Samimi, and F. Gutierrez, "Millimeter wave mobile communications for 5G celluar: It will work!," *IEEE Access*, Vol. 1, 335–349, May 2013.